A shear-shear torsional beam model for nonlinear aeroelastic analysis of tower buildings

G. Piccardo[1], F.Tubino[1], A.Luongo[2]

[1]DICCA, Polytechnic Scool, University of Genoa, Via Montallegro 1, 16145 Genoa, Italy
[2] M&MoCS, University of L'Aquila, Zona Ind.le di Bazzano, Loc. Monticchio, 67100 L'Aquila, Italy
email: giuseppe.piccardo@unige.it, federica.tubino@unige.it, angelo.luongo@univaq.it

Cite this article as: Piccardo G., Tubino F., Luongo A. A shear-shear torsional beam model for nonlinear aeroelastic analysis of tower buildings. *Journal of Applied Mathematics and Physics (ZAMP)* (2015), 66(4). 1895-1913.

ABSTRACT: In this paper, an equivalent one-dimensional beam model immersed in a three-dimensional space is proposed to study the aeroelastic behaviour of tower buildings: linear and nonlinear dynamics are analyzed through a simple but realistic physical modeling of the structure and of the load. The beam is internally constrained, so that it is capable to experience shear strains and torsion only. The elasto-geometric and inertial characteristics of the beam are identified from a discrete model of three-dimensional frame, via a homogenization process. The model accounts for the torsional effect induced by the rotation of the floors around the tower axis; the macroscopic shear strain is produced by bending of the columns, accompanied by negligible rotation of the floors. Nonlinear aerodynamic forces are evaluated through the quasi-steady theory. The first aim is to investigate the effect of mechanical and aerodynamic coupling on the critical galloping conditions. Furthermore, the role of aerodynamic nonlinearities on the galloping postcritical behavior is analyzed through a perturbation solution which permits to obtain a reduced one-dimensional dynamical system, capable of capturing the essential dynamics of the problem.

KEY WORDS: equivalent beam model, homogenization procedure, aeroelastic instability, perturbation approach

1 INTRODUCTION

Tower buildings are usually slender structures very sensitive to wind-induced vibrations. If these structures are lightweight and with low damping capacity, they can be potentially subjected to aeroelastic instability phenomena.

Finite Element techniques are not in question for the detailed design and analysis of beam systems (*e.g.*, [1,2]); nevertheless, in recent years there is a renewed and growing interest in the technical literature about simple models which can be useful for preliminary design analysis. Semi-analytical approaches may offer interpretive advantages compared to purely numerical modeling in terms of structural global behavior. In this context, different models have been proposed in the literature to analyze the distribution of the external forces on high-rise buildings [3,4], to estimate their dynamic characteristics [5-10], and to estimate their dynamic response to wind loadings [11-14]. An approximated method to determine displacements and member forces of multiple-bay bi-dimensional frames using continuum models is presented in [15]. The possibility of adopting equivalent one-dimensional coarse models representative of the global behavior of three-dimensional systems is deeply analyzed, for instance, in [16].

On the other hand, if the tower building is sufficiently slender, it is prone to phenomena of aeroelastic instability, such as galloping (*e.g.*, [17,18]). The galloping is usually dealt with section models or ideally homogeneous beam, in which the shape of the cross-section governs the stability of the problem, whereas the mechanics is usually modeled in a very simplified way; problems similar to galloping instability can be found in wave propagation (*e.g.*, [19]). The importance of the possible resonance between modes involved (generally two, flexural-flexural or flexural-torsional modes) has been highlighted (*e.g.*, [20]) pointing out the limitations of a treatment that involves only the crosswind vibrations as in the well-known Den Hartog criterion [21]. But the joint analysis of aeroelastic actions and mechanical coupling between different motion components of the building has never been highlighted to the best knowledge of the authors.

In this paper, a continuous model of beam immersed in a three-dimensional space and capable to experience shear strains and torsion only is proposed by using a heuristic identification method similar to the one presented, for instance, in [22,23]; a comprehensive description of these class of models using variational techniques can be found in [24]. The paper's aim is to study the critical and postcritical aeroelastic behavior of slender tower-buildings. Based on results of literature related to fluid-structure interaction phenomena [21], according to which the most important nonlinearities are usually of aerodynamic nature, it is assumed here that the structure behaves as a linear system, while the aerodynamic forces nonlinearly depend on torsional rotation and velocities. A coarse linear model is adopted for the frame, modeled as a three-dimensional shear-type, capable to experience translations of the floors transverse to the axis, and twist rotations around the same axis, via a homogenization process. A rigorous proof of this convergence could be obtained by means of the methods discussed in [25]. In the proposed model, the macroscopic shear strain is produced by bending of the columns, accompanied by negligible rotation of rigid floors, prevented by the high axial stiffness of the columns. The torsional effect induced by the rotation of the floors around the tower axis is included. Thus, starting from the desired macroscopic kinematics, the microscopic kinematics is assumed to be known following an approach already present in the pioneering work of Gabrio Piola [26]. The limits of this procedure are related to the possibility that the assumed microscopic kinematics could not be respected: in this case, the model should be improved by the addition of suitable kinematic parameters (as a *generalized continuum*) in order to take into account possible microscopic motions neglected in the proposed approach. From a general point of view, the proposed model of shear-shear torsional beams can be considered as one-dimensional Cosserat continuum with internal constraints (*e.g.*, [27]). Aerodynamic forces are evaluated through the classic quasi-steady theory considering nonlinear terms up to the third order. The fundamental problem for the aeroelastic behavior is derived, including kinematics relationships, balance equations, elastic law and external forces. Based on the proposed beam model, the critical wind velocity and the post-critical

behavior of tower buildings can be determined taking into account the mechanical and aerodynamic coupling between torsional and transversal vibrations. The linearized problem allows to perform a linear bifurcation analysis in order to analyze critical instability conditions as a function of the mechanical and aerodynamic characteristics of the structure. The post-critical analysis is carried out applying the Multiple Scale Method. As a sample system, a square building excited along a symmetry axis is considered. The effect of mechanical eccentricity on critical galloping conditions and the influence of the aerodynamic nonlinearities on the post-critical amplitude are studied.

2 THE STRUCTURAL MODEL

A shear-beam is characterized by shear strains much larger than flexural ones: it is a coarse model for shear-type frames under planar excitation transverse to the axis. In this Section, the kinematics of this model is described (Sect 2.1), then its dynamics (Sect 2.2); finally, a constitutive law is derived via a homogenization procedure (Sect 2.3).

2.1 Kinematics

The shear-beam is considered as a one-dimensional polar continuum whose points, in the reference configuration, lie on the segment $s\in[0,\ell]$ (assumed to be coincident with the *centroidal axis* of the underlying three-dimensional model). The beam is endowed with a rigid local structure, described by mutually orthogonal unit vectors attached to the material points. Let $\bar{\mathbf{a}}_1$, $\bar{\mathbf{a}}_2$, $\bar{\mathbf{a}}_3$ be the triad in the reference configuration, with $\bar{\mathbf{a}}_1$ aligned on the beam axis (Fig. 1), and let $\mathbf{a}_1(s,t)$, $\mathbf{a}_2(s,t)$, $\mathbf{a}_3(s,t)$ be the transformed triad in the current configuration, occupied at time t (Fig. 2). The beam is assumed internally constrained, namely unflexurable and clamped at one end. Therefore $\bar{\mathbf{a}}_1\equiv\mathbf{a}_1$ and $\mathbf{a}_2=\bar{\mathbf{a}}_2\cos\theta+\bar{\mathbf{a}}_3\sin\theta$, $\mathbf{a}_3=-\bar{\mathbf{a}}_2\sin\theta+\bar{\mathbf{a}}_3\cos\theta$, where θ is the *twist* angle (Fig. 2). Consequently, the current configuration of the beam is described by four scalar configuration variables, the displacement of the centroidal axis $\mathbf{u}:=u_1(s,t)\,\bar{\mathbf{a}}_1+u_2(s,t)\,\bar{\mathbf{a}}_2+u_3(s,t)\,\bar{\mathbf{a}}_3$ and the twist $\theta(s,t)$.

The vectors $\mathbf{e}:=\mathbf{R}^T\mathbf{u}'$, $\boldsymbol{\kappa}:=\theta'(s,t)\bar{\mathbf{a}}_1$, where $\mathbf{R}$ represents the rotation tensor around $\bar{\mathbf{a}}_1$ and a dash denotes differentiation with respect to *s*, are defined as the *strain vector* and *torsion*, respectively; moreover, $\mathbf{e}=\varepsilon\bar{\mathbf{a}}_1+\boldsymbol{\gamma}$, with ε the axial and $\boldsymbol{\gamma}$ the shear strain. By letting $\boldsymbol{\gamma}:=\gamma_2\bar{\mathbf{a}}_2+\gamma_3\bar{\mathbf{a}}_3$, $\boldsymbol{\kappa}:=\kappa_t\bar{\mathbf{a}}_1$, under the hypothesis of small displacement gradients, the scalar components in the current configurations are:

$$\begin{aligned}\varepsilon &= u_1'\\ \gamma_2 &= u_2'\\ \gamma_3 &= u_3'\\ \kappa_t &= \theta'\end{aligned} \tag{1}$$

Geometrical boundary conditions at the clamped end *D* require:

$$u_{1D}=u_{2D}=u_{3D}=\theta_D=0 \tag{2}$$

2.2 Dynamics

External forces $\mathbf{p}:=p_1(s,t)\,\bar{\mathbf{a}}_1+p_2(s,t)\,\bar{\mathbf{a}}_2+p_3(s,t)\,\bar{\mathbf{a}}_3$ and couples $\mathbf{c}:=c(s,t)\,\bar{\mathbf{a}}_1$ act on the beam (Fig. 1). The internal contact force $\mathbf{t}:=N(s,t)\mathbf{a}_1+T_2(s,t)\mathbf{a}_2+T_3(s,t)\mathbf{a}_3$ and the couple $\mathbf{m}:=M_t\mathbf{a}_1$ are assumed as stress measures, and referred as the *stress forces* (constituted by the normal *N* and shear forces T_2,T_3) and the *torsional moment*. Equilibrium in the current configuration requires $\mathbf{m}'+\mathbf{u}'\times\mathbf{t}+\mathbf{c}=\mathbf{0}$ and $\mathbf{t}'+\mathbf{p}=\mathbf{0}$; considering small displacement gradients and small displacements, the linearized scalar balance equations read:

$$\begin{aligned}N'+p_1&=0\\ T_2'+p_2&=0\\ T_3'+p_3&=0\\ M_t'+c&=0\end{aligned} \tag{3}$$

The mechanical boundary conditions, to be satisfied at the free end *E*, are:

$$
\begin{aligned}
N_{1E} - P_{1_E} &= 0 \\
T_{2E} - P_{2_E} &= 0 \\
T_{3E} - P_{3E} &= 0 \\
M_{tE} - C_E &= 0
\end{aligned}
\tag{4}
$$

where $\mathbf{P}_E := P_{1E}(t)\,\bar{\mathbf{a}}_1 + P_{2E}(t)\,\bar{\mathbf{a}}_2 + P_{3E}(t)\,\bar{\mathbf{a}}_3$ and $\mathbf{C}_E := C_E(t)\,\bar{\mathbf{a}}_1$ are a known force and a couple, respectively, acting at E. In this paper distributed and concentrated forces in axial direction (characterized by the subscript 1) are neglected; therefore, the normal force N is set to zero.

External forces are here distinguished in (a) *aerodynamic*, (b) *inertial*, and (c) *damping* forces; accordingly:

$$
\begin{aligned}
\mathbf{p} &= \mathbf{p}_a - m\ddot{\mathbf{u}} - \xi_u \dot{\mathbf{u}} \\
\mathbf{c} &= \mathbf{c}_a - I_1 \ddot{\theta}\bar{\mathbf{a}}_1 - \xi_\theta \dot{\theta}\bar{\mathbf{a}}_1 \\
\mathbf{P}_E &= \mathbf{P}_{Ea} - M_E \ddot{\mathbf{u}}_E - \Xi_{uE}\dot{\mathbf{u}}_E \\
\mathbf{C}_E &= \mathbf{C}_{Ea} - \left(I_{1E}\ddot{\theta}_E - \Xi_{\theta E}\dot{\theta}_E \right)\bar{\mathbf{a}}_1
\end{aligned}
\tag{5}
$$

where the index a denotes aerodynamic; m is the mass per unit length of the beam; I_1 is the inertia mass moment of the cross section with respect to $\bar{\mathbf{a}}_1$; M_E is a lumped mass, possibly attached at the free end of the beam, and I_{1E} its inertia moment. *External* damping forces are taken proportional to the masses, via the damping coefficients ξ, Ξ; internal damping, if any, must be accounted via a visco-elastic constitutive law. Note that the centroidal axis was taken as coincident with the beam axis in order to simplify the expression of the inertia forces.

2.3 Hyperelastic law

Let us consider a generic column c of axis $\bar{\mathbf{a}}_1$, and principal inertia axes $\bar{\mathbf{a}}_2$, $\bar{\mathbf{a}}_3$, clamped at both ends C and B, undergoing a displacement $\mathbf{u}_B = u_{1B}\,\bar{\mathbf{a}}_1 + u_{2B}\,\bar{\mathbf{a}}_2 + u_{3B}\,\bar{\mathbf{a}}_3$ and a twist θ_B, assigned at B (Fig. 3). In the framework of the Euler-Bernoulli beam linear theory, the column experiences a displacement field:

$$\mathbf{u}(s)=u_{1B}g(s)\bar{\mathbf{a}}_1+f(s)(u_{2B}\bar{\mathbf{a}}_2+u_{3B}\bar{\mathbf{a}}_3) \tag{6}$$

where s is an abscissa with origin at C, and the functions g and f are given by:

$$g(s):=s/h \qquad\qquad f(s):=3(s/h)^2-2(s/h)^3 \tag{7}$$

h being the length of the column. The elastic energy stored by the column is given by:

$$W_c=\frac{1}{2}\int_0^h\left(EA\varepsilon^2+GJ_t\kappa_1^2+EI_{2c}\kappa_2^2+EI_{3c}\kappa_3^2\right)\mathrm{ds} \tag{8}$$

where ε is the axial strain and κ_i (i=1,2,3) are the curvatures of the column:

$$\varepsilon=u_1' \qquad \kappa_1=\theta' \qquad \kappa_2=-u_3'' \qquad \kappa_3=-u_2'' \tag{9}$$

Taking into account Eqs. (6)-(9), the column elastic energy W_c can be expressed as a function of its end-section displacements as follows:

$$W_c=\frac{1}{2}\left(k_c^a u_{1B}^2+k_{2c}^f u_{2B}^2+k_{3c}^f u_{3B}^2+k_c^t\theta_B^2\right) \tag{10}$$

where $k_c^a:=EA/h$ is the axial stiffness, $k_{2c}^f:=12EI_{3c}/h^3$, $k_{3c}^f:=12EI_{2c}/h^3$ are flexural stiffnesses, and $k_c^t:=GJ_t/h$ is the torsional stiffness.

Let us now analyze a cell made of two adjacent floors, parallel to the $\bar{\mathbf{a}}_2,\bar{\mathbf{a}}_3$ plane, connected by N columns of equal height h aligned along $\bar{\mathbf{a}}_1$. The relative motion of the upper floor with respect to the lower one is considered, consisting in a translation $\mathbf{u}_G=u_{1G}\bar{\mathbf{a}}_1+u_{2G}\bar{\mathbf{a}}_2+u_{3G}\bar{\mathbf{a}}_3$, with G the centroid, and in a rotation θ around the axis $\bar{\mathbf{a}}_1$. By linear kinematics, the displacement of the top point of the i-th column, of coordinates x_{2i}, x_{3i}, is $\mathbf{u}_i=u_{1i}\bar{\mathbf{a}}_1+u_{2i}\bar{\mathbf{a}}_2+u_{3i}\bar{\mathbf{a}}_3$, where:

$$\begin{aligned} u_{1i}&=u_{1G}\\ u_{2i}&=u_{2G}-\theta x_{3i}\\ u_{3i}&=u_{3G}+\theta x_{2i}\end{aligned} \tag{11}$$

Assuming that all the columns have principal axes aligned with $\bar{\mathbf{a}}_2, \bar{\mathbf{a}}_3$, the elastic energy of the N columns can be expressed as:

$$W := \sum_{i=1}^{N} W_i \tag{12}$$

where W_i represents the elastic energy of the i-th column. Substituting Eq. (10) (by replacing c and B with i) into Eq. (12), the elastic energy of the cell is given by:

$$W := \frac{1}{2} \sum_{i=1}^{N} \left\{ k_i^a u_{1i}^2 + k_{2i}^f u_{2i}^2 + k_{3i}^f u_{3i}^2 + k_i^t \theta^2 \right\} \tag{13}$$

Then, substituting Eq. (11) into Eq. (13), one obtains the following expression of the elastic energy as a function of the displacements of the centroid (u_{1G}, u_{2G}, u_{3G}) and of the rotation θ:

$$W = \frac{1}{2} \sum_{i=1}^{N} \left[k_i^a u_{1G}^2 + k_{2i}^f \left(u_{2G} - \theta x_{3i} \right)^2 + k_{3i}^f \left(u_{3G} + \theta x_{2i} \right)^2 + k_i^t \theta^2 \right] \tag{14}$$

The axial force necessary to enforce such displacements is:

$$N = \frac{\partial W}{\partial u_{1G}} = \sum_{i=1}^{N} k_i^a u_{1G} \tag{15}$$

If no axial forces are applied, then $N = 0$, and therefore the centroidal axial displacement must vanish ($u_{1G} = 0$).

The elastic energy of the cell is thus given by:

$$W = \frac{1}{2} \sum_{i=1}^{N} \left[k_{2i}^f \left(u_{2G} - \theta x_{3i} \right)^2 + k_{3i}^f \left(u_{3G} + \theta x_{2i} \right)^2 + k_i^t \theta^2 \right] \tag{16}$$

The constitutive law of the coarse model is obtained by expressing:

$$u_{2G}=\gamma_2 h \quad u_{3G}=\gamma_3 h \quad \theta=\kappa_t h \tag{17}$$

Furthermore, let us express the elastic energy per unit length of the equivalent beam as $\phi=W/h$. By substituting Eq. (17) into Eq. (16), we obtain:

$$\phi=\frac{h}{2}\sum_{i=1}^{N}\left[k_{2i}^{f}\left(\gamma_2-\kappa_t x_{3i}\right)^2+k_{3i}^{f}\left(\gamma_3+\kappa_t x_{2i}\right)^2+k_i^t\kappa_t^2\right] \tag{18}$$

By the Green law:

$$T_2=\frac{\partial\phi}{\partial\gamma_2}, \quad T_3=\frac{\partial\phi}{\partial\gamma_3}, \quad M_t=\frac{\partial\phi}{\partial\kappa_t} \tag{19}$$

a linear constitutive law is deduced:

$$\begin{aligned} T_2&=hK_2^f\gamma_2-hx_{3F}K_2^f\kappa_t \\ T_3&=hK_3^f\gamma_3+hx_{2F}K_3^f\kappa_t \\ M_t&=h\left(K^t+K^{tf}\right)\kappa_t-hx_{3F}K_2^f\gamma_2+hx_{2F}K_3^f\gamma_3 \end{aligned} \tag{20}$$

In Eq. (20), $K_2^f:=\sum_{i=1}^{N}k_{2i}^f$ and $K_3^f:=\sum_{i=1}^{N}k_{3i}^f$ are the total flexural stiffnesses, $K^t:=\sum_{i=1}^{N}k_i^t$ is the total torsional stiffness, $K^{tf}:=\sum_{i=1}^{N}\left(k_{2i}^f x_{3i}^2+k_{3i}^f x_{2i}^2\right)$ is the contribution to the torsional stiffness given by the flexural stiffness of the columns, x_{2F} and x_{3F} are the coordinates of the center F of the flexural stiffness:

$$x_{2F}:=\frac{1}{K_3^f}\sum_{i=1}^{N}k_{3i}^f x_{2i} \qquad x_{3F}:=\frac{1}{K_2^f}\sum_{i=1}^{N}k_{2i}^f x_{3i} \tag{21}$$

3 THE AERODYNAMIC MODEL

Aerodynamic forces are modeled based on the quasi-steady theory, assuming that the flow-induced forces acting on a moving cylinder can be predicted adopting the expression pertinent to a fixed cylinder in which the asymptotic flow velocity is substituted with the flow-cylinder relative velocity

(*e.g.*, [28]). This requirement is often met at high reduced velocity U_r, *i.e.* $U_r = U/(f_c \cdot b) > 20-30$ [21], where U is the modulus of the mean wind velocity $\mathbf{U}$, f_c is the cylinder's oscillation frequency and b is a reference size of the cylinder cross-section (*e.g.*, the diameter or the side). Even if technicians involved in the study of structures subjected to aeroelastic actions may consider the quasi-steady approach as too simplistic and often unrealistic, it remains an irreplaceable, though approximate, simple tool to perform preliminary predictive analyses before performing more sophisticated ones.

Under the assumption of the quasi-steady theory, the aerodynamic forces $\mathbf{p}_a$ and couple $\mathbf{c}_a$ acting on the beam can be expressed as a function of the relative wind velocity as follows [29]:

$$\begin{aligned}\mathbf{p}_a &= \frac{1}{2}\rho_a V b\left(c_d(\alpha)\mathbf{V} + c_l(\alpha)\mathbf{a}_1 \times \mathbf{V}\right)\\ \mathbf{c}_a &= \frac{1}{2}\rho_a V^2 b^2 c_m(\alpha)\mathbf{a}_1\end{aligned} \tag{22}$$

where ρ_a is the air density, $\mathbf{V}:=\mathbf{U}-\dot{\mathbf{u}}$ is the relative wind velocity, difference between the absolute (mean) velocity of the wind $\mathbf{U}$ and the local velocity of the structure $\dot{\mathbf{u}}=\dot{u}_2\mathbf{a}_2+\dot{u}_3\mathbf{a}_3$, $V=\|\mathbf{V}\|$ is the modulus of the relative wind velocity; furthermore $c_d(\alpha)$, $c_l(\alpha)$, $c_m(\alpha)$ are aerodynamic coefficients, called drag, lift and moment coefficients, respectively, evaluated for the instantaneous angle of attack α:

$$\alpha = \arctan\left(\frac{\mathbf{V}\cdot\mathbf{a}_3}{\mathbf{V}\cdot\mathbf{a}_2}\right) = \beta - \theta + \arctan\left(\frac{\mathbf{V}\cdot(\mathbf{a}_1\times\mathbf{U})}{\mathbf{V}\cdot\mathbf{U}}\right) \tag{23}$$

being β the angle of incidence of the absolute wind velocity $\mathbf{U}$ with respect to the reference configuration, Fig. 4.

The components of the aerodynamic forces in the wind reference basis (drag p_{ad}, lift p_{al}, moment p_{am}) are defined as follows:

$$
\begin{aligned}
p_{ad} &= \mathbf{p}_a \cdot \frac{\mathbf{U}}{U} \\
p_{al} &= \mathbf{p}_a \cdot \frac{(\mathbf{a}_1 \times \mathbf{U})}{U} \\
p_{am} &= c_a
\end{aligned}
\tag{24}
$$

Their approximation at the third order is obtained from Eq.(22) by a power series expansion of the relative wind velocity **V** and the angle of attack α, Eq. (23), with respect to the mean value U and the angle of incidence β, respectively, considering small rotations θ and structural velocities $\dot{\mathbf{u}}$ (see, *e.g.*, [28]), and can be expressed as follows:

$$
p_{a\varepsilon} = \frac{1}{2}\rho_a b \left\{ \begin{array}{l}
U\left(C_{\varepsilon 2}\dot{u}_2 + C_{\varepsilon 3}\dot{u}_3 + UC_{\varepsilon t}\theta\right) + \\
\left(C_{\varepsilon 22}\dot{u}_2^2 + C_{\varepsilon 33}\dot{u}_3^2 + U^2 C_{\varepsilon tt}\theta^2 + UC_{\varepsilon 2t}\dot{u}_2\theta + UC_{\varepsilon 3t}\dot{u}_3\theta + C_{\varepsilon 23}\dot{u}_2\dot{u}_3\right) + \\
+ \dfrac{1}{U}\left(\begin{array}{l}
C_{\varepsilon 222}\dot{u}_2^3 + C_{\varepsilon 333}\dot{u}_3^3 + C_{\varepsilon 223}\dot{u}_2^2\dot{u}_3 + C_{\varepsilon 233}\dot{u}_2\dot{u}_3^2 + U^3 C_{\varepsilon ttt}\theta^3 + U^2 C_{\varepsilon tt2}\theta^2\dot{u}_2 + \\
+ U^2 C_{\varepsilon tt3}\theta^2\dot{u}_3 + UC_{\varepsilon t22}\theta\dot{u}_2^2 + UC_{\varepsilon t33}\theta\dot{u}_3^2 + UC_{\varepsilon t23}\theta\dot{u}_2\dot{u}_3
\end{array} \right)
\end{array} \right\} \quad (\varepsilon = d, l, m)
\tag{25}
$$

where the coefficients C are defined in Appendix A.

The components (p_{a2}, p_{a3}) of the aerodynamic forces in the structural reference basis ($\bar{\mathbf{a}}_2, \bar{\mathbf{a}}_3$) are related to the forces in the wind reference basis (p_{ad}, p_{al}) through a simple rotation law (Fig. 4):

$$
\begin{aligned}
p_{a2} &= p_{ad}\cos\beta - p_{al}\sin\beta \\
p_{a3} &= p_{ad}\sin\beta + p_{al}\cos\beta
\end{aligned}
\tag{26}
$$

Thus, the components of the forces in the structural reference basis p_{a2}, p_{a3} can be defined through expressions analogous to Eq. (25), (ε = 2,3), with coefficients given by:

$$
\begin{aligned}
C_{a2ijk} &= C_{dijk}\cos\beta - C_{lijk}\sin\beta \\
C_{a3ijk} &= C_{dijk}\sin\beta + C_{lijk}\cos\beta
\end{aligned}
\qquad (i,j,k = 2,3,t)
\tag{27}
$$

where one, two or three subscripts *i*,*j*,*k* are taken into consideration depending on the order of the corresponding coefficient.

Resulting aeroelastic forces are expressed as the sum of linear, quadratic and cubic terms, as in Eq. (25).

4 THE FUNDAMENTAL PROBLEM

The fundamental problem is governed by the kinematic relationships (1), (2), the balance equations (3), (4), with external forces given by Eq.(5), and the elastic law (20). Starting from the kinematic relationships and the balance equations, the equations of motion may be expressed as follows:

$$\begin{aligned} &hK_2^f u_2'' - hx_{3F}K_2^f \theta'' + p_{a2} - m\ddot{u}_2 - c_2\dot{u}_2 = 0 \\ &hK_3^f u_3'' + hx_{2F}K_3^f \theta'' + p_{a3} - m\ddot{u}_3 - c_3\dot{u}_3 = 0 \\ &h\left(K^t + K^{tf}\right)\theta'' - hx_{3F}K_2^f u_2'' + hx_{2F}K_3^f u_3'' + c_a - I_1\ddot{\theta} - c_\theta\dot{\theta} = 0 \end{aligned} \tag{28}$$

where the aerodynamic forces p_{a2}, p_{a3}, c_a are given by Eq.(25).

In absence of external forces at the free end *E*, the boundary conditions are given by:

$$\begin{aligned} &u_2(0) = u_3(0) = \theta(0) = 0 \\ &hK_2^f u_2'(\ell) - hx_{3F}K_2^f \theta'(\ell) = 0 \\ &hK_3^f u_3'(\ell) + hx_{2F}K_3^f \theta'(\ell) = 0 \\ &h\left(K^t + K^{tf}\right)\theta'(\ell) - hx_{3F}K_2^f u_2'(\ell) + hx_{2F}K_3^f u_3'(\ell) = 0 \end{aligned} \tag{29}$$

By direct inspection, the exact solution of the boundary value problem (28)-(29) is expressed as follows:

$$\begin{aligned} u_2(s,t) &= \sin\left(\frac{\pi}{2}\frac{s}{l}\right) q_2(t) \\ u_3(s,t) &= \sin\left(\frac{\pi}{2}\frac{s}{l}\right) q_3(t) \\ \theta(s,t) &= \sin\left(\frac{\pi}{2}\frac{s}{l}\right) q_t(t) \end{aligned} \tag{30}$$

Introducing the nondimensional parameters:

$$\tilde{t}=\omega_3 t,\ \tilde{q}_2=\frac{q_2}{b},\ \tilde{q}_3=\frac{q_3}{b},\ \tilde{q}_t=q_t,\ \xi_2=\frac{c_2}{2m\omega_2},\ \xi_3=\frac{c_3}{2m\omega_3},$$
$$\xi_\theta=\frac{c_\theta}{2I_1\omega_\theta},\ \tilde{x}_{2F}=\frac{x_{2F}}{b},\ \tilde{x}_{3F}=\frac{x_{3F}}{b},\ \alpha_{23}=\frac{\omega_2}{\omega_3},\ \alpha_{\theta 3}=\frac{\omega_\theta}{\omega_3},\tag{31}$$
$$\eta=\frac{I_1}{mb^2},\ \mu=\frac{U}{\omega_3 b},\ \nu=\frac{1}{2}\frac{\rho_a b^2}{m}$$

being ω_2, ω_3 and ω_θ the circular frequencies of the building in the uncoupled case (*i.e.*, symmetrical cross-section with respect to the reference axes) given by [18]:

$$\omega_2^2=\frac{hK_2^f}{m}\left(\frac{\pi}{2\ell}\right)^2,\ \omega_3^2=\frac{hK_3^f}{m}\left(\frac{\pi}{2\ell}\right)^2,\ \omega_\theta^2=\frac{h\left(K^t+K^{tf}\right)}{I_1}\left(\frac{\pi}{2\ell}\right)^2\tag{32}$$

the resulting non-dimensional system of second-order ordinary differential equations can be written in the following matrix form:

$$\mathbf{M}\ddot{\tilde{\mathbf{q}}}+\mathbf{C}_s\dot{\tilde{\mathbf{q}}}+\mathbf{K}_s\tilde{\mathbf{q}}=-\mu\mathbf{C}_a\dot{\tilde{\mathbf{q}}}-\mu^2\mathbf{K}_a\tilde{\mathbf{q}}+\mathbf{f}_2\left(\tilde{\mathbf{q}},\tilde{\mathbf{q}};\mu\right)+\mathbf{f}_3\left(\tilde{\mathbf{q}},\tilde{\mathbf{q}},\tilde{\mathbf{q}};\mu\right)\tag{33}$$

where $\tilde{\mathbf{q}}$ is the vector of the non-dimensional principal coordinates, $\mathbf{M}$, $\mathbf{C}_s$, $\mathbf{K}_s$ are the structural mass, damping and stiffness matrixes:

$$\tilde{\mathbf{q}}=\begin{Bmatrix}\tilde{q}_2\\ \tilde{q}_3\\ \tilde{q}_t\end{Bmatrix}\quad \mathbf{M}=\begin{bmatrix}1&0&0\\0&1&0\\0&0&\eta\end{bmatrix}\quad \mathbf{C}_s=\begin{bmatrix}2\xi_2\alpha_{23}&0&0\\0&2\xi_3&0\\0&0&2\xi_\theta\alpha_{\theta 3}\eta\end{bmatrix}\quad \mathbf{K}_s=\begin{bmatrix}\alpha_{23}^2&0&-\tilde{x}_{3F}\alpha_{23}^2\\0&1&\tilde{x}_{2F}\\-\tilde{x}_{3F}\alpha_{23}^2&\tilde{x}_{2F}&\alpha_{\theta 3}^2\eta\end{bmatrix}$$

(34)

Furthermore, $\mu\mathbf{C}_a$ and $\mu^2\mathbf{K}_a$ are the aerodynamic damping and stiffness matrixes:

$$\mathbf{C}_a=\nu\begin{bmatrix}-C_{a22}&-C_{a23}&0\\-C_{a32}&-C_{a33}&0\\-C_{at2}&-C_{at3}&0\end{bmatrix}\quad \mathbf{K}_a=\nu\begin{bmatrix}0&0&-C_{a2t}\\0&0&-C_{a3t}\\0&0&-C_{att}\end{bmatrix}\tag{35}$$

Finally, the vectors $\mathbf{f}_2$ and $\mathbf{f}_3$ are the quadratic and cubic aerodynamic force vectors:

$$\mathbf{f}_2(\tilde{\mathbf{q}},\dot{\tilde{\mathbf{q}}};\mu)=\frac{8}{3\pi}\nu\begin{Bmatrix} C_{a222}\dot{\tilde{q}}_2^2+C_{a233}\dot{\tilde{q}}_3^2+\mu^2C_{a2tt}\tilde{q}_t^2+\mu C_{a22t}\dot{\tilde{q}}_2\tilde{q}_t+\mu C_{a23t}\dot{\tilde{q}}_3\tilde{q}_t+C_{a223}\dot{\tilde{q}}_2\dot{\tilde{q}}_3 \\ C_{a322}\dot{\tilde{q}}_2^2+C_{a333}\dot{\tilde{q}}_3^2+\mu^2C_{a3tt}\tilde{q}_t^2+\mu C_{a32t}\dot{\tilde{q}}_2\tilde{q}_t+\mu C_{a33t}\dot{\tilde{q}}_3\tilde{q}_t+C_{a323}\dot{\tilde{q}}_2\dot{\tilde{q}}_3 \\ C_{at22}\dot{\tilde{q}}_2^2+C_{at33}\dot{\tilde{q}}_3^2+\mu^2C_{attt}\tilde{q}_t^2+\mu C_{at2t}\dot{\tilde{q}}_2\tilde{q}_t+\mu C_{at3t}\dot{\tilde{q}}_3\tilde{q}_t+C_{at23}\dot{\tilde{q}}_2\dot{\tilde{q}}_3 \end{Bmatrix}$$

$$\mathbf{f}_3(\tilde{\mathbf{q}},\dot{\tilde{\mathbf{q}}},\tilde{\mathbf{q}};\mu)=\frac{3}{4}\frac{\nu}{\mu}\begin{Bmatrix} \left(\begin{array}{l} C_{a2222}\dot{\tilde{q}}_2^3+C_{a2333}\dot{\tilde{q}}_3^3+C_{a2223}\dot{\tilde{q}}_2^2\dot{\tilde{q}}_3+C_{a2233}\dot{\tilde{q}}_2\dot{\tilde{q}}_3^2+\mu^3C_{a2ttt}\tilde{q}_t^3+\mu^2C_{a2tt2}\tilde{q}_t^2\dot{\tilde{q}}_2+ \\ \mu^2C_{a2tt3}\tilde{q}_t^2\dot{\tilde{q}}_3+\mu C_{a2t22}\tilde{q}_t\dot{\tilde{q}}_2^2+\mu C_{a2t33}\tilde{q}_t\dot{\tilde{q}}_3^2+\mu C_{a2t23}\tilde{q}_t\dot{\tilde{q}}_2\dot{\tilde{q}}_3 \end{array}\right) \\ \left(\begin{array}{l} C_{a3222}\dot{\tilde{q}}_2^3+C_{a3333}\dot{\tilde{q}}_3^3+C_{a3223}\dot{\tilde{q}}_2^2\dot{\tilde{q}}_3+C_{a3233}\dot{\tilde{q}}_2\dot{\tilde{q}}_3^2+\mu^3C_{a3ttt}\tilde{q}_t^3+\mu^2C_{a3tt2}\tilde{q}_t^2\dot{\tilde{q}}_2+ \\ \mu^2C_{a3tt3}\tilde{q}_t^2\dot{\tilde{q}}_3+\mu C_{a3t22}\tilde{q}_t\dot{\tilde{q}}_2^2+\mu C_{a3t33}\tilde{q}_t\dot{\tilde{q}}_3^2+\mu C_{a3t23}\tilde{q}_t\dot{\tilde{q}}_2\dot{\tilde{q}}_3 \end{array}\right) \\ \left(\begin{array}{l} C_{at222}\dot{\tilde{q}}_2^3+C_{at333}\dot{\tilde{q}}_3^3+C_{at223}\dot{\tilde{q}}_2^2\dot{\tilde{q}}_3+C_{at233}\dot{\tilde{q}}_2\dot{\tilde{q}}_3^2+\mu^3C_{atttt}\tilde{q}_t^3+\mu^2C_{attt2}\tilde{q}_t^2\dot{\tilde{q}}_2+ \\ \mu^2C_{attt3}\tilde{q}_t^2\dot{\tilde{q}}_3+\mu C_{att22}\tilde{q}_t\dot{\tilde{q}}_2^2+\mu C_{att33}\tilde{q}_t\dot{\tilde{q}}_3^2+\mu C_{att23}\tilde{q}_t\dot{\tilde{q}}_2\dot{\tilde{q}}_3 \end{array}\right) \end{Bmatrix} \tag{36}$$

5 LINEAR BIFURCATION ANALYSIS

The linearized reduced equations of motion (33) can be rewritten in the following state-space form:

$$\dot{\mathbf{x}}=\mathbf{G}\mathbf{x} \tag{37}$$

$\mathbf{x}=\left\{\tilde{q}_2 \quad \tilde{q}_3 \quad \tilde{q}_t \quad \dot{\tilde{q}}_2 \quad \dot{\tilde{q}}_3 \quad \dot{\tilde{q}}_t\right\}^{\mathrm{T}}$ being the state-space vector and **G** the state-space matrix:

$$\mathbf{G}=\begin{bmatrix} \mathbf{0} & \mathbf{I} \\ -\mathbf{M}^{-1}\mathbf{K} & -\mathbf{M}^{-1}\mathbf{C} \end{bmatrix} \qquad \mathbf{C}=\mathbf{C}_s+\mu\mathbf{C}_a \qquad \mathbf{K}=\mathbf{K}_s+\mu^2\mathbf{K}_a \tag{38}$$

From Eq.(38) it should be noted that the total damping of the structure is proportional to the nondimensional wind velocity μ, which acts as a bifurcation parameter. Linear bifurcation analysis is carried out by evaluating the complex eigenvalues and eigenvectors of the state-space matrix **G** as functions of μ.

The classic Den Hartog criterion corresponds to the critical velocity μ_{DH} of the sole crosswind degree of freedom, $\tilde{q}_3$, and it is achieved when β=0 and **C**(2,2)=0:

$$\mu_{DH}=\frac{-2\xi_3}{\nu\left(c_d+c_l'\right)} \tag{39}$$

6 POST-CRITICAL ANALYSIS

The nonlinear equation of motion can be expressed in the state-space form as follows:

$$\dot{\mathbf{x}}=\mathbf{G}\mathbf{x}+\varepsilon\mathbf{F}_2(\mathbf{x},\mathbf{x};\mu)+\varepsilon^2\mathbf{F}_3(\mathbf{x},\mathbf{x},\mathbf{x};\mu) \tag{40}$$

where ε is a dimensionless small parameter and $\mathbf{F}_2$ and $\mathbf{F}_3$ represent, respectively, the quadratic and cubic forcing functions:

$$\mathbf{F}_2(\mathbf{x},\mathbf{x};\mu)=\begin{Bmatrix}\mathbf{0}\\ \mathbf{f}_2\end{Bmatrix} \qquad \mathbf{F}_3(\mathbf{x},\mathbf{x},\mathbf{x};\mu)=\begin{Bmatrix}\mathbf{0}\\ \mathbf{f}_3\end{Bmatrix} \tag{41}$$

Assuming a small perturbation of μ around its critical value μ_0, $\mu=\mu_0+\varepsilon^2\hat{\mu}$, the stiffness and damping matrices may be expressed as:

$$\mathbf{K}=\mathbf{K}_0+\varepsilon^2\hat{\mu}\mathbf{K}_2 \qquad \mathbf{C}=\mathbf{C}_0+\varepsilon^2\hat{\mu}\mathbf{C}_2 \tag{42}$$

where:

$$\begin{aligned}\mathbf{K}_0&=\mathbf{K}_s+\mu_0^2\mathbf{K}_a & \mathbf{K}_2&=2\mu_0\mathbf{K}_a\\ \mathbf{C}_0&=\mathbf{C}_s+\mu_0\mathbf{C}_a & \mathbf{C}_2&=\mathbf{C}_a\end{aligned} \tag{43}$$

Thus, the bifurcation parameter can also be made explicit in the state-space matrix **G**:

$$\mathbf{G}=\mathbf{G}_0+\varepsilon^2\hat{\mu}\mathbf{G}_2 \tag{44}$$

where:

$$\mathbf{G}_0=\begin{bmatrix}\mathbf{0} & \mathbf{I}\\ -\mathbf{M}^{-1}\mathbf{K}_0 & -\mathbf{M}^{-1}\mathbf{C}_0\end{bmatrix} \qquad \mathbf{G}_2=\begin{bmatrix}\mathbf{0} & \mathbf{0}\\ -\mathbf{M}^{-1}\mathbf{K}_2 & -\mathbf{M}^{-1}\mathbf{C}_2\end{bmatrix} \tag{45}$$

In order to apply the Multiple Scale Method [30], the solution is expanded as:

$$\mathbf{x}=\mathbf{x}_0+\varepsilon\mathbf{x}_1+\varepsilon^2\mathbf{x}_2 \tag{46}$$

After introducing two independent time scales $t_0:=t$ and $t_2:=\varepsilon^2 t$, the derivative with respect to the time assumes the expression $\mathrm{d}/\mathrm{d}t=\mathrm{d}_0+\varepsilon^2\mathrm{d}_2$, where $\mathrm{d}_i=\partial/\partial t_i$ (i=0,2). As a consequence, the perturbation equations read as:

$$\begin{aligned}
&\varepsilon^0 && \mathrm{d}_0\mathbf{x}_0-\mathbf{G}_0\mathbf{x}_0=\mathbf{0}\\
&\varepsilon^1 && \mathrm{d}_0\mathbf{x}_1-\mathbf{G}_0\mathbf{x}_1=\mathbf{F}_2\left(\mathbf{x}_0,\mathbf{x}_0;\mu_0\right)\\
&\varepsilon^2 && \mathrm{d}_0\mathbf{x}_2-\mathbf{G}_0\mathbf{x}_2=-\mathrm{d}_2\mathbf{x}_0+\hat{\mu}\mathbf{G}_2\mathbf{x}_0+2\mathbf{F}_2\left(\mathbf{x}_0,\mathbf{x}_1;\mu_0\right)+\mathbf{F}_3\left(\mathbf{x}_0,\mathbf{x}_0,\mathbf{x}_0;\mu_0\right)
\end{aligned} \tag{47}$$

Eq. $(47)_1$ admits the generating solution:

$$\mathbf{x}_0=A\left(t_2\right)\mathbf{u}_0\mathrm{e}^{\mathrm{i}\omega t_0}+cc \tag{48}$$

where i is the imaginary unit, $\mathbf{u}_0$ is the right critical eigenvector of $\mathbf{G}_0$ and *cc* denotes the complex conjugate.

Substituting Eq. (48) into Eq. $(47)_2$, the following equation is obtained:

$$\mathrm{d}_0\mathbf{x}_1-\mathbf{G}_0\mathbf{x}_1=A^2\mathrm{e}^{2i\omega t_0}\mathbf{F}_2\left(\mathbf{u}_0,\mathbf{u}_0;\mu_0\right)+A\bar{A}\mathbf{F}_2\left(\mathbf{u}_0,\bar{\mathbf{u}}_0;\mu_0\right)+cc \tag{49}$$

where the overbar denotes complex conjugate.

The particular solution of Eq. (49) is given by:

$$\mathbf{x}_1=A^2\mathbf{z}_2\mathrm{e}^{2i\omega t_0}+A\bar{A}\mathbf{z}_0+cc \tag{50}$$

where $\mathbf{z}_0$ and $\mathbf{z}_2$ are solutions of the following equations:

$$\begin{aligned}
&\left(2i\omega\mathbf{I}-\mathbf{G}_0\right)\mathbf{z}_2=\mathbf{F}_2\left(\mathbf{u}_0,\mathbf{u}_0;\mu_0\right)\\
&-\mathbf{G}_0\mathbf{z}_0=\mathbf{F}_2\left(\mathbf{u}_0,\bar{\mathbf{u}}_0;\mu_0\right)
\end{aligned} \tag{51}$$

Substituting Eq. (50) into Eq. $(47)_3$, one obtains:

$$\mathrm{d}_0\mathbf{x}_2-\mathbf{G}_0\mathbf{x}_2=\mathbf{F}_r\mathrm{e}^{\mathrm{i}\omega t_0}+NRT+cc \tag{52}$$

where *NRT* denotes non resonant terms, while $\mathbf{F}_r$ represent the resonant forcing terms at the ε^2-order given by:

$$\mathbf{F}_r = -\mathrm{d}_2 A\mathbf{u}_0 + \hat{\mu} A\mathbf{G}_2\mathbf{u}_0 + A^2\bar{A}\left(2\mathbf{F}_2\left(\mathbf{u}_0,\mathbf{z}_2;\mu_0\right)+4\mathbf{F}_2\left(\mathbf{u}_0,\mathbf{z}_0;\mu_0\right)+3\mathbf{F}_3\left(\mathbf{u}_0,\mathbf{u}_0,\bar{\mathbf{u}}_0;\mu_0\right)\right) \tag{53}$$

The solvability of Eq. (52) is enforced by imposing the condition:

$$\mathbf{v}_0^{\mathrm{T}}\mathbf{F}_r = 0 \tag{54}$$

being $\mathbf{v}_0$ the conjugate critical left eigenvector of $\mathbf{G}_0$.

From Eq. (54), the amplitude modulation equation is derived:

$$\dot{A} = \hat{\mu} A c_1 + c_2 A^2 \bar{A} \tag{55}$$

where the coefficients c_1 and c_2 are given by:

$$\begin{aligned} c_1 &= \mathbf{v}_0^{\mathrm{T}}\mathbf{G}_2\mathbf{u}_0 \\ c_2 &= 2\mathbf{v}_0^{\mathrm{T}}\mathbf{F}_2\left(\mathbf{u}_0,\mathbf{z}_2;\mu_0\right)+4\mathbf{v}_0^{\mathrm{T}}\mathbf{F}_2\left(\mathbf{u}_0,\mathbf{z}_0;\mu_0\right)+3\mathbf{v}_0^{\mathrm{T}}\mathbf{F}_3\left(\mathbf{u}_0,\mathbf{u}_0,\bar{\mathbf{u}}_0;\mu_0\right) \end{aligned} \tag{56}$$

By introducing the polar form $A = 1/2 a e^{\mathrm{i}\theta}$ and separating real and imaginary parts of c_1 and c_2 coefficients ($c_i = c_{iR} + \mathrm{i}c_{iI}$, i=1,2), the modulation equation in the real amplitude a is obtained:

$$\dot{a} = \hat{\mu} a c_{1R} + \frac{1}{4} a^3 c_{2R} \tag{57}$$

The stationary amplitude a is estimated by imposing $\dot{a} = 0$:

$$a = 2\sqrt{-\frac{c_{1R}}{c_{2R}}\hat{\mu}} \tag{58}$$

The approximate perturbation solution of Eq. (40) is thus obtained from Eq. (46) reabsorbing the ε parameter.

7 NUMERICAL APPLICATIONS

In order to appreciate the effective importance of the coupling between mechanical and aerodynamic terms, a numerical application is proposed. The building considered has an external square shape; the columns are supposed to be disposed symmetrically with respect to $\bar{\mathbf{a}}_2$ axis, so that $\tilde{x}_{3F}$=0. Furthermore, it is assumed that the uncoupled natural frequencies in the two orthogonal directions are coincident (α_{23}=1). The non-dimensional coefficients ν and η are fixed as ν=0.004, η=1/6; damping ratios are set as $\xi_2=\xi_3=\xi_\theta$=0.01. The mean wind velocity is assumed to be aligned with $\bar{\mathbf{a}}_2$, so that β=0. The aerodynamic coefficients for the square section are chosen according to [31] and [32] (c_d = 2.09, c_l = 0, c_m = 0, c_d' = 0, c_l' = -5.69, c_m' = 0.196, c_d'' = -18.35, c_l'' = 0, c_m'' = 0, c_d''' = 0, c_l''' = 2337, c_m''' = 130.7).

At first, a linear bifurcation analysis is carried out and the effects on critical conditions of the eccentricity between flexural and inertia center $\tilde{x}_{2F}$, and of the torsional-to-shear frequency ratio $\alpha_{\theta 3}$ are studied. As a second step, a specific class of tower buildings is considered and the role of the different kinds of nonlinearities on the post-critical behaviour is analyzed.

7.1 Linear bifurcation analysis

Linear bifurcation analysis is carried out by analyzing the complex eigenvalues and eigenvectors of the state-space matrix as functions of the non-dimensional mean wind velocity μ (considered as the bifurcation parameter), of the eccentricity between flexural and inertia center $\tilde{x}_{2F}$, and of the torsional-to-shear frequency ratio $\alpha_{\theta 3}$.

Figure 5 plots the complex eigenvalues on varying the non-dimensional mean wind velocity μ (the arrow indicates the increase of μ) for different values of the involved parameters ((a) $\tilde{x}_{2F}$=0.1, $\alpha_{\theta 3}$=1.3,..2 from black to grey; (b) $\alpha_{\theta 3}$=1.3, $\tilde{x}_{2F}$=0,..0.2 from black to grey). Figure 5(c) provides a schematic representation of the corresponding eigenvectors, showing that the first couple of

eigenvalues ($\lambda_{1,2}$) is related to an alongwind mode, while the other two couples ($\lambda_{3,4}$, $\lambda_{5,6}$) correspond to coupled lateral-torsional vibrations. It is evident that the couple of eigenvalues associated with the alongwind mode ($\lambda_{1,2}$) have imaginary part independent of μ and a real part that decreases on increasing μ (the aerodynamic damping is proportional to μ, while the stiffness is independent of μ), whereas it is independent of $\alpha_{\theta 3}$ and $\tilde{x}_{2F}$. On the contrary, the other two couples of eigenvalues (referred to potentially coupled crosswind-torsional vibrations) are characterized by an imaginary part that slightly depends on μ and a real part that is strongly affected by μ. In particular, the increase of μ has a stabilizing effect (the real part decreases) on the stable couple of modes ($\lambda_{3,4}$) while the unstable couple of modes ($\lambda_{5,6}$) has a real part that increases with increasing μ. The imaginary part of the unstable eigenvalues ($\lambda_{5,6}$) is almost independent of $\alpha_{\theta 3}$ for $\tilde{x}_{2F}$ =0.1, whereas it is slightly affected by $\tilde{x}_{2F}$; the imaginary part of the stable eigenvalue ($\lambda_{3,4}$) is influenced by $\alpha_{\theta 3}$ but almost independent of $\tilde{x}_{2F}$.

Figure 6 plots the real parts of the eigenvalues as functions of the non-dimensional mean wind velocity μ, for different values of the involved parameters ((a) $\tilde{x}_{2F}$ =0.1, $\alpha_{\theta 3}$=1.3,..1.9; (b) $\alpha_{\theta 3}$=1.3, $\tilde{x}_{2F}$ =0,..0.2). As already deduced from Fig. 5, the real part of the eigenvalues associated with crosswind and torsional motions is affected by the aerodynamic damping terms. In particular, there exists a critical value of velocity, μ_{cr}, at which the real part of the unstable couple of eigenvalues ($\lambda_{5,6}$) crosses the zero value; it is influenced by both $\tilde{x}_{2F}$ and $\alpha_{\theta 3}$. For the example here examined, the critical value decreases when the eccentricity diminishes and the frequency ratio increases (*i.e.* when the coupling between lateral and torsional vibrations tends to vanish).

Figure 7 shows the absolute value of the crosswind u_{03} (a) and torsional $u_{0\theta}$ (b) components of the critical eigenvector $\mathbf{u}_0$ as functions of $\alpha_{\theta 3}$ and $\tilde{x}_{2F}$ (the alongwind component is not plotted since it is null). It clearly shows that the critical mode is a coupled vibration in the crosswind ($\bar{\mathbf{a}}_3$) and

torsional directions. In particular, the vibration is purely crosswind ($u_{0\theta}$=0) for negligible eccentricity between the flexural and inertia center ($\tilde{x}_{2F}$ close to zero); on increasing $\tilde{x}_{2F}$, the coupling between torsional and crosswind vibrations becomes remarkable. Furthermore, the coupling increases on decreasing the frequency ratio, $\alpha_{\theta 3}\rightarrow 1$. In any case, the coupling is significant even for large frequency ratios if the eccentricity $\tilde{x}_{2F}$ is sufficiently large.

Figure 8 shows the ratio between the critical non-dimensional mean wind velocity and the Den Hartog limit value (39) as a function of $\alpha_{\theta 3}$ and $\tilde{x}_{2F}$. It is evident that the coupling between shear and torsion has always a stabilizing effect, causing a significant increase of the critical wind velocity with respect to the classic Den Hartog criterion.

7.2 Post-critical analysis

As a sample numerical application, the stationary amplitude has been evaluated for a specific case, in which $\tilde{x}_{2F}$ =0.05 is assumed. In this particular case, the right critical eigenvector is given by $\mathbf{u}_0$= $\{0 \quad 0.65 \quad 0.29+0.02\mathrm{i} \quad 0 \quad -0.64\mathrm{i} \quad 0.02-0.28\mathrm{i}\}^{\mathrm{T}}$. The role of the different aerodynamic terms is investigated by comparing the full model with suitable reduced models, obtained neglecting the quadratic aerodynamic terms, or taking into account only the aerodynamic cubic terms proportional to the crosswind degree of freedom (which are the only ones present in a purely 1 degree-of-freedom crosswind galloping model), or considering the classic (Den Hartog) crosswind uncoupled galloping. Figure 9 plots the stationary amplitude of oscillation deduced by Eq. (58). The full nonlinear model shows post-critical amplitudes remarkably lower than the reduced model with only cubic nonlinearities in $\dot{\tilde{q}}_3^3$. The solution obtained neglecting the quadratic aerodynamic terms is not reported since it almost perfectly coincides with the complete solution of the full model, demonstrating that the quadratic terms have a negligible role in this case and are not responsible for this reduction effect. The coupling between torsion and lateral vibrations causes a noteworthy modification of the post-

critical behaviour with respect to the purely crosswind case. As already observed from Fig. 8, the critical velocity for the classic uncoupled crosswind galloping may be significantly lower than the one evaluated for coupled vibrations, and the corresponding post-critical amplitudes are higher than ones arising in coupled cases using the full model.

In order to check the accuracy of the perturbation solution in predicting the post-critical stationary amplitude of vibration, a numerical integration of the nonlinear equations of motion (33) has been carried out, imposing an initial condition $\tilde{\mathbf{q}}(0)=\{0 \quad 0.1 \quad 0\}^{\mathrm{T}}$ and assuming a non-dimensional mean wind velocity $\mu=1.2\mu_{\mathrm{cr}}$, (μ_{cr} =1.58). Figure 10 shows the steady-state numerical time histories $\tilde{q}_\alpha$ (α=3,*t*) ($\tilde{q}_2$ is not reported since alongwind vibrations are not significant for the examined case), together with the corresponding steady-state amplitude $a/2\ u_{0\alpha}$ (α=3,*t*; gray straight line), with *a* estimated from Eq. (58) ($\hat{\mu}=\mu-\mu_{cr}$ =0.316): the perturbation solution provides a reliable estimate of the stationary amplitude of the crosswind and torsional components of motion. Figure 11 plots the steady-state trajectory of a point located at a corner of the square building ($\tilde{x}_2=\tilde{x}_3$ =0.5), comparing the numerical solution with the perturbation one: the two solutions are almost coincident; furthermore, the coupling between crosswind vibration and torsion causes a non-negligible motion of the selected point also along $\bar{\mathbf{a}}_2$ direction.

8 CONCLUSIONS AND PROSPECTS

The main novelty of this paper consists in modeling a wind-excited shear-type three-dimensional frame as an equivalent one-dimensional beam. The model is linear in accounting for inertial, elastic and damping forces, but nonlinear in describing fluid-structure interactive forces. It allows to take into account the mechanical coupling between shear and torsion due to the lack of symmetry in the mechanical properties of the structure. This makes it possible to study the linear and nonlinear dynamic interaction between elastic and non-conservative forces based on a realistic physical

modeling of the structure and the load. In the analyzed examples simple codimension-1 Hopf bifurcations occur. The use of Multiple Scale perturbation method permits to obtain a reduced one-dimensional dynamical system ruling the main dynamics on the center manifold. It is obviously well different and richer than (usual) technical single degree-of-freedom section model, since it may include all the three components of the tower-building motion (and not only the crosswind lateral displacement as in the classic vertical galloping).

As a sample application, the galloping analysis of a square building excited by the wind along a symmetry axis has been carried out. It should be noted that, although the requirements of the quasi-steady theory (demanding a high slenderness of the tower-building) can be met with difficulty, it has been adopted in similar cases in the literature (*e.g.*, [17],[18],[33],[34]). Anyway, it allows to carry out a preliminary analysis of the system stability, which may precede more detailed (and complicated) aeroelastic experimental tests and simulations. The influence of the lack of symmetry and of the coupling between shear and torsion on the critical galloping conditions has been studied. In the case here presented, this coupling always has a stabilizing effect, since it produces an increase of the critical wind velocity and a reduction of the post-critical amplitude of oscillation with respect to the purely crosswind galloping. Comparisons between results of a numerical integration of the equations of motion and the perturbation solution confirm the validity of the analytical approach in estimating the post-critical stationary amplitude.

Based on the equivalent model here introduced, the critical wind velocity and the post-critical behavior can be estimated for different building shapes when the angle of incidence of the mean wind is varying (*i.e.* $\beta \neq 0$), recovering the possible influence of alongwind vibrations. Furthermore, the postcritical behaviour can be analyzed by applying the Multiple Scale Method directly to the partial differential equations of motion (as, *e.g.*, done in [35]). Finally, the procedure can be extended to include mechanical nonlinearities (simply by using Biot strain and, for instance, the results found in [36],[37]) and non-homogeneous beams, possibly bearing lumped masses on the top.

ACKNOWLEDGMENTS

This work was supported by the Italian Ministry of Education, Universities and Research (MIUR) through the PRIN co-financed program ’Dynamics, Stability and Control of Flexible Structures’ (grant number 2010MBJK5B).

APPENDIX A

The coefficients defining the aerodynamic forces $p_{a\varepsilon}$ (ε=*d, l, m*) in Eq. (25) can be expressed as:

$$
\begin{aligned}
&C_{\varepsilon 2}=c_{\varepsilon 2}\sin\beta-2c_{\varepsilon 1}\cos\beta \qquad C_{\varepsilon 3}=-c_{\varepsilon 2}\cos\beta-2c_{\varepsilon 1}\sin\beta \qquad C_{\varepsilon t}=-c'_{\varepsilon 1}\\
&C_{\varepsilon 22}=c_{\varepsilon 1}-c_{\varepsilon 2}\cos\beta\sin\beta+c_{\varepsilon 3}\left(\sin\beta\right)^2 \qquad C_{\varepsilon 33}=c_{\varepsilon 1}+c_{\varepsilon 2}\cos\beta\sin\beta+c_{\varepsilon 3}\left(\cos\beta\right)^2\\
&C_{\varepsilon tt}=\frac{1}{2}c''_{\varepsilon 1} \qquad C_{\varepsilon 2t}=2c'_{\varepsilon 1}\cos\beta-c'_{\varepsilon 2}\sin\beta \qquad C_{\varepsilon 3t}=2c'_{\varepsilon 1}\sin\beta+c'_{\varepsilon 2}\cos\beta\\
&C_{\varepsilon 23}=c_{\varepsilon 2}\cos 2\beta-c_{\varepsilon 3}\sin 2\beta \qquad C_{\varepsilon 222}=c_{\varepsilon 4}\left(\sin\beta\right)^3 \qquad C_{\varepsilon 333}=-c_{\varepsilon 4}\left(\cos\beta\right)^3\\
&C_{\varepsilon 223}=-3c_{\varepsilon 4}\cos\beta\left(\sin\beta\right)^2 \qquad C_{\varepsilon 233}=3c_{\varepsilon 4}\left(\cos\beta\right)^2\sin\beta \qquad C_{\varepsilon ttt}=-\frac{1}{6}c'''_{\varepsilon 1}\\
&C_{\varepsilon tt2}=-c''_{\varepsilon 1}\cos\beta+\frac{1}{2}c''_{\varepsilon 2}\sin\beta \qquad C_{\varepsilon tt3}=-c''_{\varepsilon 1}\sin\beta-\frac{1}{2}c''_{\varepsilon 2}\cos\beta \qquad C_{\varepsilon t22}=-c'_{\varepsilon 1}-c'_{\varepsilon 3}\left(\sin\beta\right)^2+c'_{\varepsilon 2}\cos\beta\sin\beta\\
&C_{\varepsilon t33}=-c'_{\varepsilon 1}-c'_{\varepsilon 3}\left(\cos\beta\right)^2-c'_{\varepsilon 2}\cos\beta\sin\beta \qquad C_{\varepsilon t23}=-c'_{\varepsilon 2}\cos 2\beta+c'_{\varepsilon 3}\sin 2\beta
\end{aligned}
\tag{59}
$$

where the coefficients $c_{\varepsilon i}$ (ε=*d,l,m, i*=1,..4) are functions of the aerodynamic coefficients, defined as follows:

$$
\begin{aligned}
&c_{d1}=c_d \qquad c_{l1}=c_l \qquad c_{m1}=c_m\\
&c_{d2}=-c_l+c'_d \qquad c_{l2}=c_d+c'_l \qquad c_{m2}=c'_m\\
&c_{d3}=-\frac{c_d}{2}-c'_l+\frac{c''_d}{2} \qquad c_{l3}=-\frac{c_l}{2}+c'_d+\frac{c''_l}{2} \qquad c_{m3}=\frac{c''_m}{2}\\
&c_{d4}=-\frac{c_l}{2}+\frac{c'_d}{6}-\frac{c''_l}{2}+\frac{c'''_d}{6} \qquad c_{l4}=\frac{c_d}{2}+\frac{c'_l}{6}+\frac{c''_d}{2}+\frac{c'''_l}{6} \qquad c_{m4}=\frac{2}{3}c'_m+\frac{c'''_m}{6}
\end{aligned}
\tag{60}
$$

where the prime symbol denotes the derivatives of the aerodynamic coefficients with respect to the instantaneous angle of attack α, evaluated at the angle β.

The coefficients of the linear terms of the forces in the structural reference basis (C_{a22}, C_{a23}, C_{a32}, C_{a33}) are coincident with those already introduced by Piccardo et al. [38].

REFERENCES

[1] L. Greco, M. Cuomo, An implicit G1 multi patch B-spline interpolation for Kirchhoff-Love space rod, Computer Methods in Applied Mechanics and Engineering 269 (2014), 173-197.

[2] A. Cazzani, M. Malagù, E. Turco, Isogeometric analysis of plane-curved beams, Mathematics and Mechanics of Solids (2014), doi: 10.1177/1081286514531265.

[3] T. Balendra, S. Swaddiwudhipong, S-T. Quek, S-L. Lee, Approximate analysis of asymmetric buildings. Journal of Structural Engineering 110(9) (1984), 2056-2072.

[4] A. Carpinteri, G. Lacidogna, S. Puzzi, A global approach for three dimensional analysis of tall buildings, The Structural Design of Tall and Special Buildings 19 (2010), 518-536.

[5] A.K. Basu, G.Q. Dar, Dynamic characteristics of coupled wall-frame systems, Earthquake Engineering and Structural Dynamics 10 (1982), 615-631.

[6] E. Miranda, S. Taghavi, Approximate floor acceleration demands in multistory buildings. I: Formulation, Journal of Structural Engineering ASCE 131 (2005), 203-211.

[7] M. Malekinejad, R. Rahgozar, A simple analytic method for computing the natural frequencies and mode shapes of tall buildings, Applied Mathematical Modelling 36 (2012), 3419-3432.

[8] M. Malekinejad, R. Rahgozar, An analytical model for dynamic response analysis of tubular tall buildings, The Structural Design of Tall and Special Buildings 23(1) (2014), 67–80.

[9] C.L. Dym, H.E. Williams, Estimating fundamental frequencies of tall buildings, Journal of Structural Engineering ASCE 133(10) (2007), 1479-1483.

[10] C.L. Dym, Approximating frequencies of tall buildings, Journal of Structural Engineering ASCE 139(2) (2013), 288-293.

[11] C.P. Patrickson, P.P. Friedmann, Deterministic torsional building response to wind, Journal of the Structural Division 105(ST12) (1979), 2621-2637.

[12] M.A.M. Torkamani, E. Pramono, Dynamic response of tall building to wind excitation, Journal of Structural Engineering ASCE 111(4) (1985), 805-825.

[13] T. Balendra, G.K. Nathan, K.H. Kang, Deterministic model for wind-induced oscillations of buildings, Journal of Engineering Mechanics ASCE 115(1) (1989), 179-199.

[14] F. Cluni, M. Gioffrè, V. Gusella, Dynamic response of tall buildings to wind loads by reduced order equivalent shear-beam models, Journal of Wind Engineering and Industrial Aerodynamics 123 (2013), 339-348.

[15] M.J. Chajes, K.M. Romstad, D.B. McCallen, Analysis of multiple-bay frames using continuum model, J. Struct. Engrg. ASCE 119(2) (1993), 522-546.

[16] A. Luongo, D. Zulli, Mathematical Models of Beams and Cables. Wiley-ISTE, London 2013.

[17] L. Shuguo, L. Qiusheng, L. Guiqing, Q. Weilian, An evaluation of onset wind velocity for 2-D coupled galloping oscillations of tower buildings, Journal of Wind Engineering and Industrial Aerodynamics 50 (1993), 329-340.

[18] A. Luongo, D. Zulli, Parametric, external and self-excitation of a tower under turbulent wind flow, Journal of Sound and Vibration 330 (2011), 3057-3069.

[19] A. Madeo, I. Djeran-Maigre, G. Rosi, C. Silvani, The effect of fluid streams in porous media on acoustic compression wave propagation, transmission, and reflection, Continuum Mechanics and Thermodynamics 25(2-4) (2013), 173-196.

[20] A. Luongo, G. Piccardo G., Linear instability mechanisms for coupled translational galloping, Journal of Sound and Vibration 288 (2005), 1027-1047.

[21] M.P. Païdoussis, S.J. Price, E. de Langre, Fluid-Structure Interactions – Cross-flow-induced instabilities. Cambridge University Press, New York 2011.

[22] F. dell'Isola, L. Rosa, C. Woźniak, Dynamics of solids with micro periodic nonconnected fluid inclusions, Archive of Applied Mechanics 67 (1997), 215-228.

[23] F. dell'Isola, L. Rosa, C. Woźniak, A micro-structured continuum modelling compacting fluid-saturated grounds: The effects of pore-size scale parameter, Acta Mechanica 127(1-4) (1998), 165-182.

[24] D. Steigmann, G.M. Faulkner, Variational theory for spatial rods, Journal of Elasticity 33(1) (1993), 1-26.

[25] J. Alibert, P. Seppecher, F. dell'Isola, Truss modular beams with deformation energy depending on higher displacement gradients, Mathematics and Mechanics of Solids 8 (1) (2003), 51-73.

[26] F. dell'Isola, U. Andreaus, L. Placidi, At the origins and in the vanguard of peridynamics, non-local and higher gradient continuum mechanics. An underestimated and still topical contribution of Gabrio Piola, Mathematics and Mechanics of Solids (MMS), first published on February 2, 2014 as doi:10.1177/1081286513509811 (2014).

[27] M. Bîrsan, H. Altenbach, T. Sadowski, V. A. Eremeyev, D. Pietras, Deformation analysis of functionally graded beams by the direct approach, Composites Part B: Engineering 43(3) (2012), 1315-1328.

[28] G. Piccardo, L.C. Pagnini, F. Tubino, Some research perspectives in galloping phenomena: critical conditions and postcritical behavior, Continuum Mechanics and Thermodynamics DOI: 10.1007/s00161-014-0374-5 (2014).

[29] A. Luongo, D. Zulli, G. Piccardo, On the effect of twist angle on nonlinear galloping of suspended cables, Computers and Structures 87 (2009), 1003-1014.

[30] A.H. Nayfeh, D.T. Mook, Nonlinear oscillations. John Wiley & Sons, New York 1979.

[31] Y. Nakamura, T. Mizota, Torsional flutter of rectangular prisms, Journal of the Engineering Mechanics Division ASCE 101(EM2) (1975), 125-142.

[32] T. Tamura, T. Miyagi, The effect of turbulence on aerodynamic forces on a square cylinder with various corner shapes, Journal of Wind Engineering and Industrial Aerodynamics 83 (1999), 135-145.

[33] Q.S. Li, J.P. Fang, A.P. Jeary, Evaluation of 2D coupled galloping oscillations of slender structures, Computers & Structures 66(5) (1998), 513-523.

[34] M. Abdel-Rohman, Effect of unsteady wind flow on galloping of tall prismatic structures, Nonlinear Dynamics 26 (2001), 231–252.

[35] A. Luongo, G. Piccardo, A continuous approach to the aeroelastic stability of suspended cables in 1:2 internal resonance, Journal of Vibration and Control 14(2) (2008), 135-157.

[36] F. dell'Isola, L. Rosa, Perturbation methods in torsion of thin hollow Saint-Venant cylinders, Mechanics Research Communications, 23(2) (1996), 145-150.

[37] F. dell'Isola, G. Ruta, Perturbation series for shear stress in flexure of Saint-Venant cylinders with Bredt-like sections, Mechanics Research Communications 23(5) (1996), 557-564.

[38] G. Piccardo, L. Carassale, A. Freda, Critical conditions of galloping for inclined square cylinders, Journal of Wind Engineering and Industrial Aerodynamics 99(6-7) (2011), 748-756.

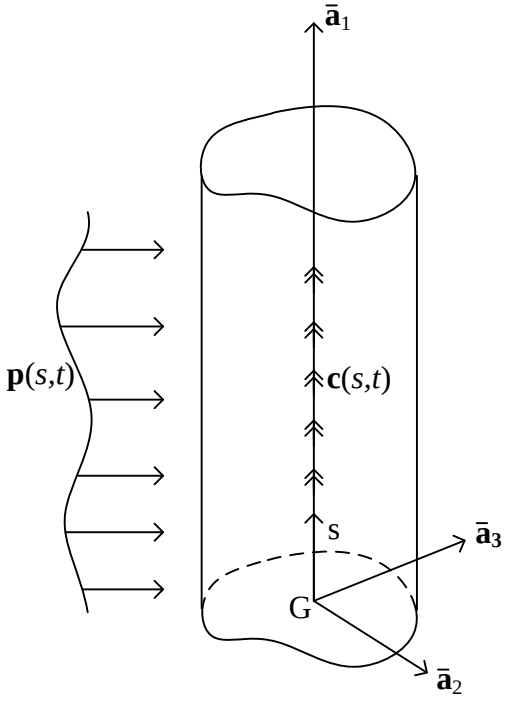

Figure 1. Tower building configuration and external loading.

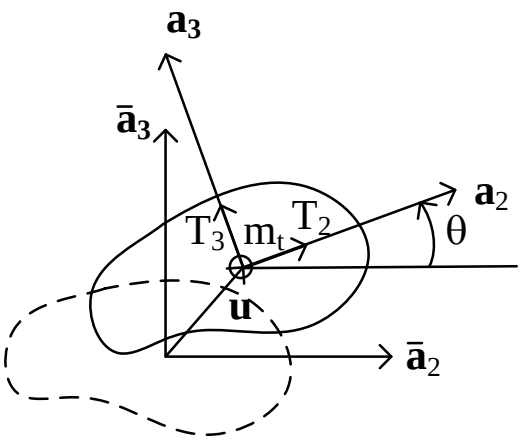

Figure 2. Tower building: reference and current bases, configuration variables and internal forces.

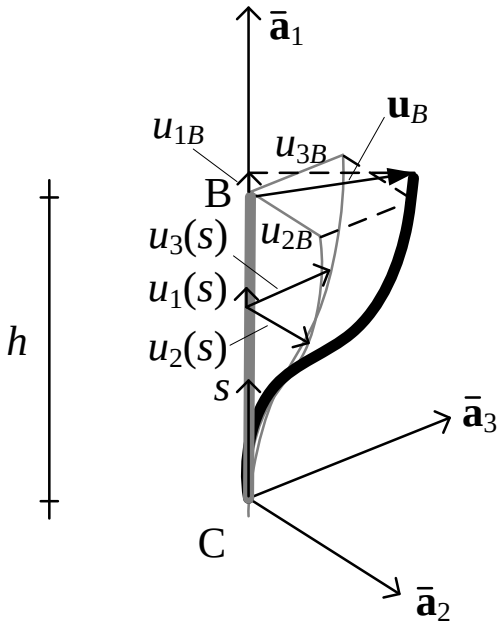

Figure 3. Single column deformation.

FIGURA MODIFICATA con u1b, CONTROLLARE se va BENE

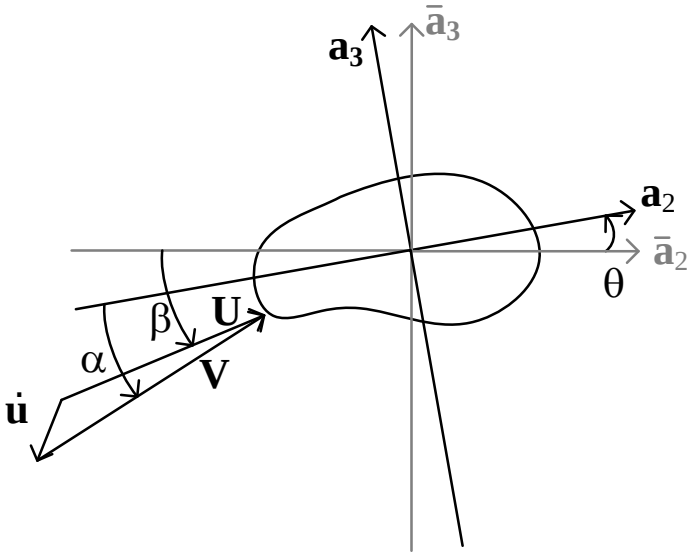

Figure 4. Absolute (**U)** and relative (**V**) velocities, aerodynamic angles.

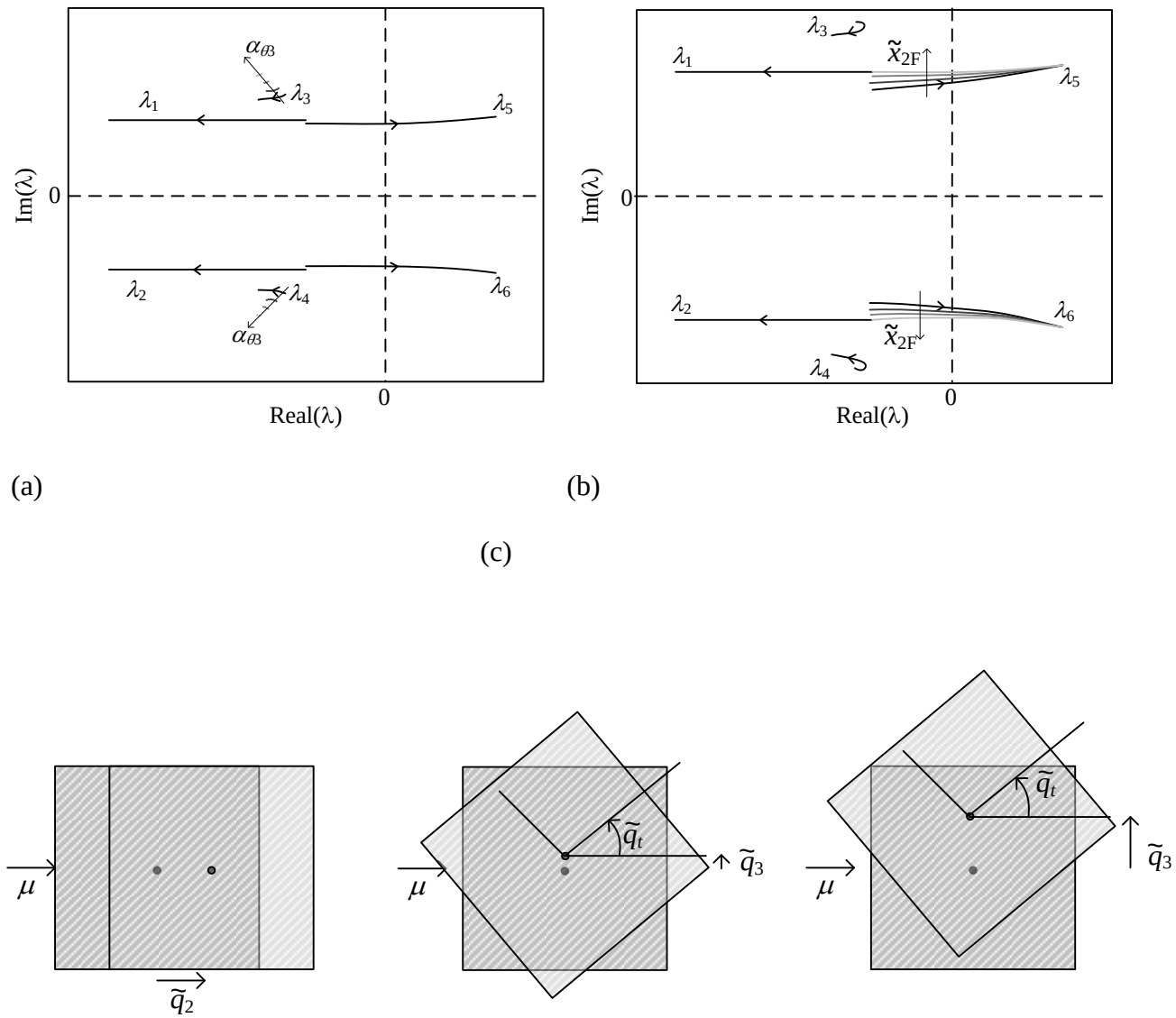

Figure 5: Complex eigenvalues ((a) $\tilde{x}_{2F}$ =0.1; (b) $\alpha_{\theta 3}$=1.3) and eigenvectors (c).

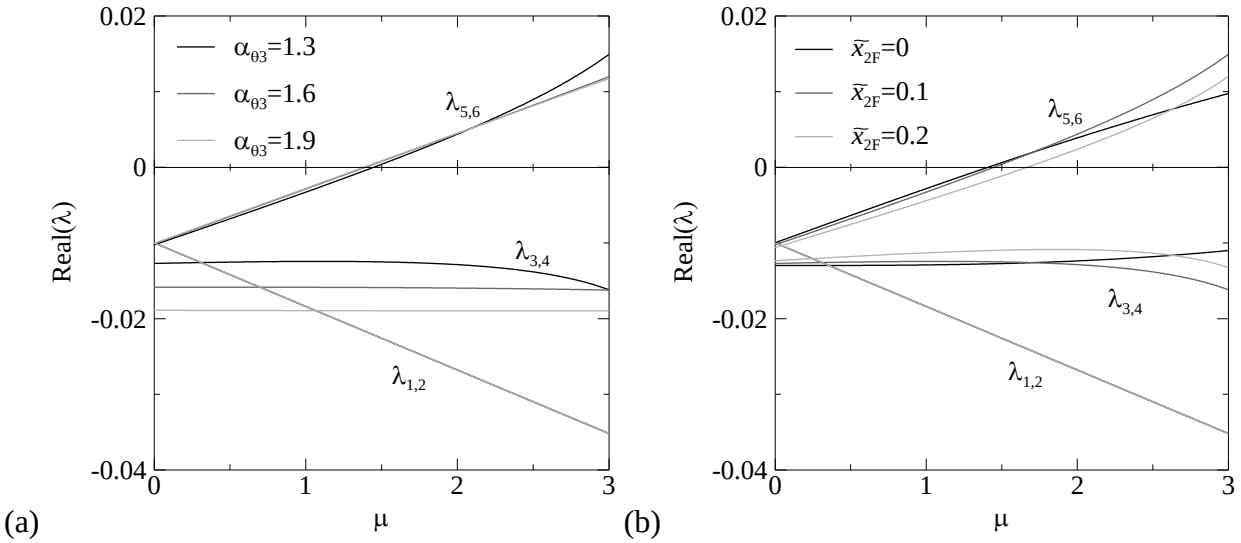

Figure 6. Real part of the eigenvalues ((a) $\tilde{x}_{2F}$ =0.1, (b) $\alpha_{\theta 3}$=1.3).

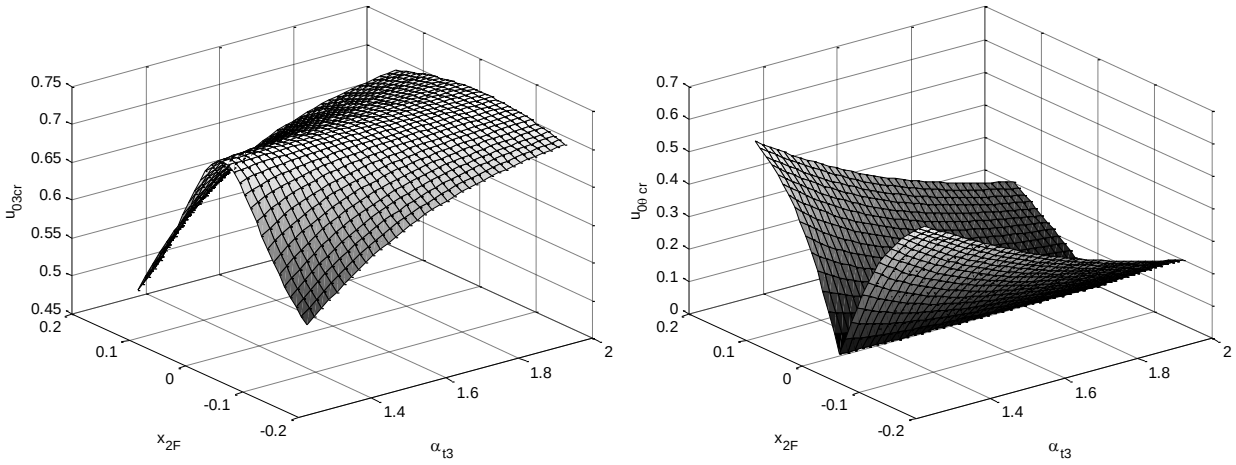

(a) (b)

Figure 7. Absolute value of the components of the critical eigenvector as functions of $\tilde{x}_{2F}$ and $\alpha_{\theta 3}$.

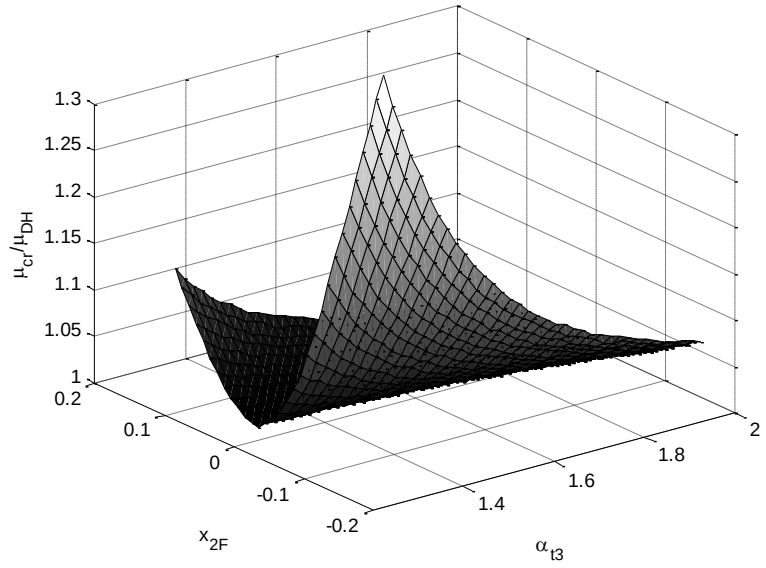

Figure 8. Ratio between the critical galloping velocity and the Den Hartog criterion as a function of $\alpha_{\theta 3}$ and $\tilde{x}_{2F}$.

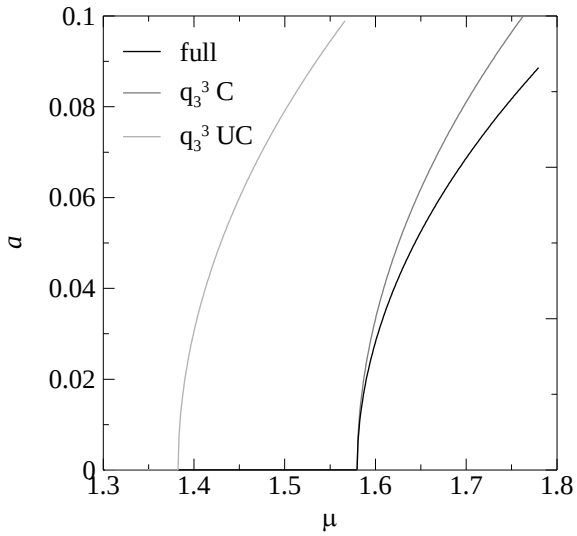

Figure 9. Postcritical amplitude: full nonlinear model (full), only cubic nonlinearities in $\dot{\tilde{q}}_3^3$ ($q_3{}^3$ C), only cubic nonlinearities in $\dot{\tilde{q}}_3^3$ and uncoupled crosswind motion ($q_3{}^3$ UC).

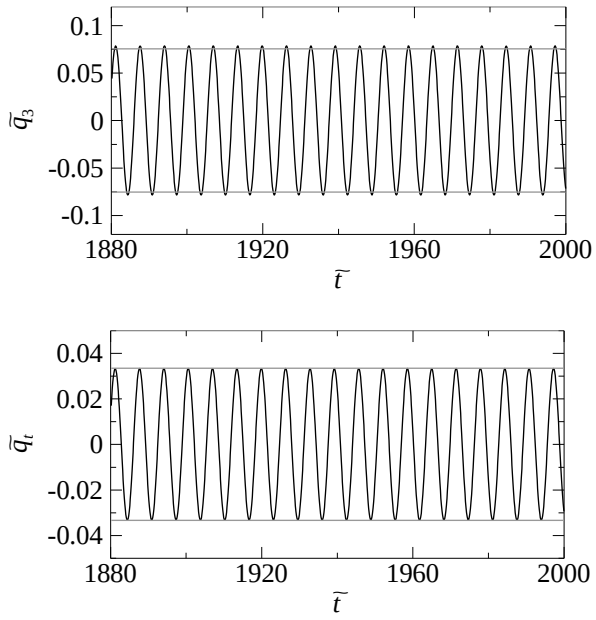

Figure 10: Steady-state time histories of the non-dimensional coordinates $\tilde{q}_3$ and $\tilde{q}_t$: comparison between numerical and analytical solution.

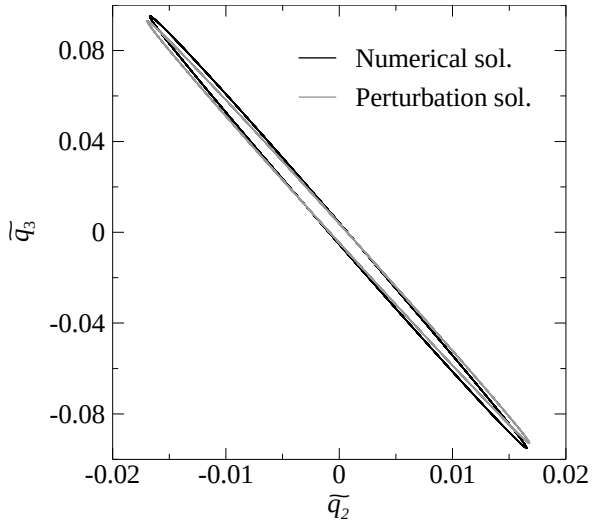

Figure 11: Steady-state trajectories of the tower-building corner point ($\tilde{x}_2 = \tilde{x}_3 = 0.5$; different scales for $\tilde{q}_2$ and $\tilde{q}_3$ axis).